Available online at www.sciencedirect.com
SCIENCE DIRECT®
PERGAMON
International Journal of Heat and Mass Transfer 46 (2003) 5087–5097
International Journal of HEAT and MASS TRANSFER
www.elsevier.com/locate/ijhmt

Quasi-homogeneous boiling nucleation on a small spherical heater in microgravity

Ho Sung Lee [a,*], Herman Merte Jr. [b], Gerold Picker [c], Johannes Straub [d]

[a] Department of Mechanical and Aeronautical Engineering, Western Michigan University, Kalamazoo, MI 49008, USA
[b] Department of Mechanical Engineering, University of Michigan, Ann Arbor, MI 48109, USA
[c] Thermo-and Aerodynamics Department, ABB Alstom Technology Ltd., CH-5405 Baden/Dattwil, Switzerland
[d] Faculty of Mechanical Engineering, Technical University of Munich, D-85748 Garching, Germany

Received 17 January 2003; received in revised form 18 June 2003

Abstract

Pool boiling experiments were conducted in the European Space Agency (ESA) multi-user facility, the bubble, drop, particle unit (BDPU) in the microgravity environment of space. A part of the study involved the heating of a small sphere immersed in R-123 to the onset of nucleate boiling. An analysis of the nucleation process is presented, based on a prior work for so-called quasi-homogeneous nucleation with a flat heater surface in microgravity. Reasonably good qualitative agreement exists between the analysis and measurements.

1. Introduction

Homogeneous and heterogeneous liquid-to-vapor nucleation has been not only of scientific and theoretical interest, related to the understanding of the fundamental mechanisms involved, but is also of practical interest for applications where boiling is to be initiated. Pure liquid can become metastable by superheating if the heat source in contact with the liquid is sufficiently smooth and no pre-existing gases or vapors are present, since the formation of a vapor nucleus requires the work of formation associated with surface tension in addition to the free energy of the phase change. The onset of the resulting transition is generally termed homogenous nucleation. If foreign solid materials in contact with the liquid contain cavities within which gases or vapors are present, with the consequence that less energy is required to form a nucleus, the resulting process is termed heterogeneous nucleation.

It has been postulated that nucleation in metastable superheated liquids is associated with the random fluctuations of energy within ensembles of molecules, until a critical size of vapor embryo is reached, from which subsequent growth can take place. Any external disturbance can cause such a nucleus to be formed prematurely in liquids, and this phenomenon is used in tracking charged particles in a hydrogen bubble chamber, for example, where highly metastable hydrogen liquid produces a visible bubble trace along the path of the particles.

Nucleation in boiling differs, in one point, from the nucleation of liquid drops or crystallization of solids from vapor, in that in the latter cases a large number of nuclei form and grow simultaneously and spontaneously within a volume or over an area, whereas with boiling nucleation one of the potential vapor nuclei randomly stimulated to grow is sufficient to dominate the ensuing process by inhibiting the formation of other potential nuclei in its neighborhood. This difference in behavior arises because of the difference in the direction of the corresponding density changes.

Whether homogeneous or heterogeneous boiling nucleation takes place in a particular situation has usually not been open to question: homogeneous nucleation requires special conditions for its onset, and is sometimes manifested by a rather dynamic subsequent behavior, depending on the amount of superheated

* Corresponding author. Tel.: +1-269-387-6536; fax: +1-219-387-3358.
E-mail address: hosung.lee@wmich.edu (H.S. Lee).

0017-9310/$ - see front matter © 2003 Elsevier Ltd. All rights reserved.
doi:10.1016/S0017-9310(03)00379-X

Nomenclature

A	heater surface area	r	spherical coordinate
B	arbitrary constant in Eq. (22) (approximately 1/3)	s	seconds
		x	plane coordinate
C	coefficient for nucleation rate. Eq. (24)	t	time
G	Gibbs number. Eq. (25)	t^*	delay time between the onset of power to heater and nucleation
g	gravity		
G_T	temperature derivative of Gibbs number	T^*	temperature at nucleation
J	steady state nucleation rate (nuclei/m^3 s)	$\dot{T}$	rate of change of temperature
K	constant (denoted as J/n'', Eq. (29); Also Kelvin	T_x	temperature gradient
		T_s	saturation temperature
k	thermal conductivity; Boltzmann constant	T_∞	bulk temperature
m	mass of molecule; m	u'''	volumetric internal heat generation rate
n, n''	number of nuclei, and per unit area. Eq. (26)	V	volume of thermistor heater
N_l	number density of liquid molecules	α	thermal diffusivity
P	input power	$\theta(T - T_\infty)$	temperature rise above the initial ambient
P_v	vapor pressure	σ	surface tension
P_l	liquid pressure	τ	time

liquid and the heat capacity of the containing vessel. The effects of potentially premature nucleation sites inherent on solid metallic surfaces is eliminated by superheating liquid droplets in an immiscible liquid having a sufficiently high boiling point (e.g. [2]), or by heating the solid surface in contact with the test liquid sufficiently rapidly that the heat transfer to the liquid greatly exceeds that associated with the evaporative latent heat, termed the pulse heating method with fine platinum wires, described by Skripov [10].

High superheats at nucleation have been achieved on glass surfaces by the use of convective heating of the glass, also described by Skripov. However, difficulties involved in relating the measurements obtained to the analysis of homogeneous nucleation arise because of the transient conduction and convection heat transfer taking place. These were eliminated when the opportunity arose for heating a liquid in the absence of gravity in space experiments. Results of heating R-113, with step changes at various levels of heat flux, from a flat semi-transparent gold film sputtered on a polished quartz substrate are presented by Merte and Lee [7]. For what was observed and classified as quasi-homogeneous nucleation in that work, the influence of heat flux level and system pressure, used to vary the initial bulk liquid subcooling, were described by the modification of classical homogenous nucleation theory: The heater surface superheat at nucleation increased as the heat flux increased, and decreased as the system pressure increased. However, at the highest level of heat flux used, the nucleation process reverted to heterogeneous nucleation, based on the observations that the nucleation occurred at the same fixed locations when the experiments were repeated. This is contrasted with the results at the lower levels of heat flux, where nucleation took place at different random locations when the experiments were repeated.

The opportunity arose to further test the concept of so-called quasi-homogeneous nucleation presented in Merte and Lee [7] for a different heater geometry, when pool boiling experiments were conducted in the bubble, drop, particle unit (BDPU) on the STS-78 Life and Microgravity Science (LMS) Mission in 1996 published partly in Straub [13]. The LMS mission was a re-flight of experiments flown on the IML-2 Mission in 1994, with the results reported by Straub et al. [11] and [12]. A vapor bubble was initiated in liquid R-123 using an approximate spherical heater, consisting of a thermistor coated with a smooth glass material, with a step onset of the input power. The mean thermistor heater temperature and power were measured, along with bulk liquid temperature and pressure. In the absence of gravity the heat transfer to the liquid is by pure conduction, until nucleation disturbs the liquid. This is particularly advantageous for nucleation studies in that the temperature distribution in the liquid is known at the instant of nucleation. It will be demonstrated below that the present spherical heater experiments with R-123 support the conclusions of the previous study with a flat heater and R-113.

In order to provide the explicit temperature data needed for evaluation of the nucleation process—the temperature gradients and rates of temperature change in the liquid in the vicinity of the glass surface at the

instant of nucleation, an analytical model was developed, rather than a numerical model, assuming a spherical shape for the thermistor heater and its glassy coating. The model solves the transient one-dimensional boundary-value heat conduction problem in spherical coordinates for three concentric materials, with the assumption of perfect thermal contact between the layers. The model approximates the smooth thermistor heater used in the present experiments.

The objective here is to determine the behavior of nucleation on a smooth approximately spherical solid heater, in which the heat flux or steep temperature gradient at or near the solid surface might work as a disturbance to initiate the nucleation. Basic homogeneous nucleation theory is adopted, rather than heterogeneous nucleation theory, to explain the nucleation taking place, presumed to be adjacent to the smooth solid heater. The first two authors in the work presented here conducted the analysis and calculations, while the last two authors were responsible for the experimental measurements.

2. Experiments and measurements

The experiments were performed in a pool boiling test container in the ESA multi-user facility, the BDPU on the STS-78 LMS mission. The test cell, filled with R-123, is internally spherical with a diameter of 50 mm. A photo of the glass coated thermistor used as the heater is shown in Fig. 1, with a schematic for mathematical modeling given in Fig. 2, assuming spherical symmetry as an approximation to the actual case. The thermistor, having a diameter of about 1.56 mm, provides not only the energy required for the bubble nucleation, but the measurement of its internal temperature as well. Further details are given in Straub et al. [11] and [12].

Fig. 3 shows typical measurements of the thermistor heater temperature and input power over the experimental period. Since operation in microgravity virtually eliminates natural convection in the liquid, the nucleation process can be studied using temperature distributions known at the instant of nucleation. The thermistor temperature is seen to rise to 141.2 °C at nucleation after the application of power: this also heats the surrounding stagnant liquid by transient conduction heat transfer. Nucleation takes place at approximate 13.9 s following the onset of heating, which is defined here as the nucleation delay time (t^*). The mean thermistor heater temperature of 141.2 °C corresponds to a superheat of 27.2 K for the saturation temperature of 114 °C in this run. This does not take into consideration the temperature drop across the glass coating in Fig. 1, which will be determined from the analytical model to be described in the following section. The nucleation delay time, the heater surface superheat as well as its rate of change, and the liquid temperature distribution in its vicinity at the nucleation time are important parameters in the description of the nucleation process. The imposed experimental conditions and corresponding measurements related to nucleation are listed in Table 1, columns [1–10], for selected tests. The basis for this selection will be given below. It is interesting to note in Fig. 3 that after nucleation occurs, whereby the heater temperature decreases abruptly, steady nucleate boiling sets in at a constant temperature of 130 °C.

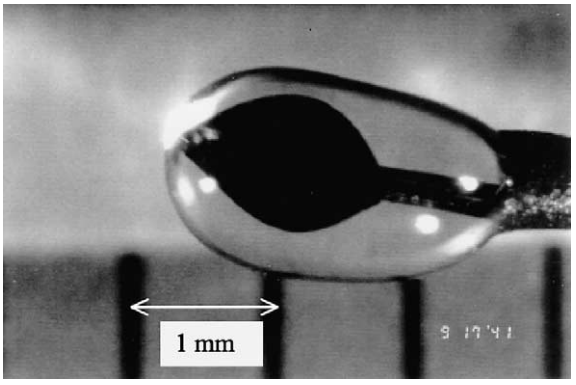

Fig. 1. Photo of glass coated thermistor used as heater.

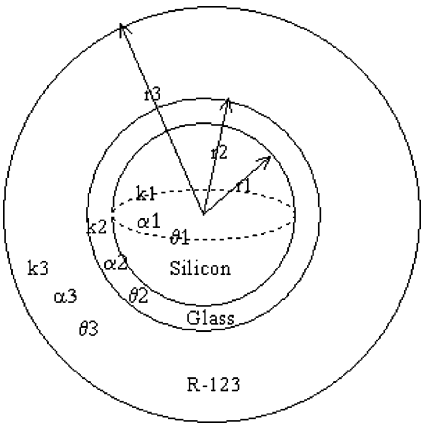

Fig. 2. Schematic of the thermistor heater for analytical model.

3. Analytical model

An analytical 1-D spherical model for three layered bodies was developed, using the existing solutions of Bulavin and Kashcheev [3], to provide the transient temperature distributions for the following case, which approximates the experimental physical circumstances used: a metal central core with internal heat generation

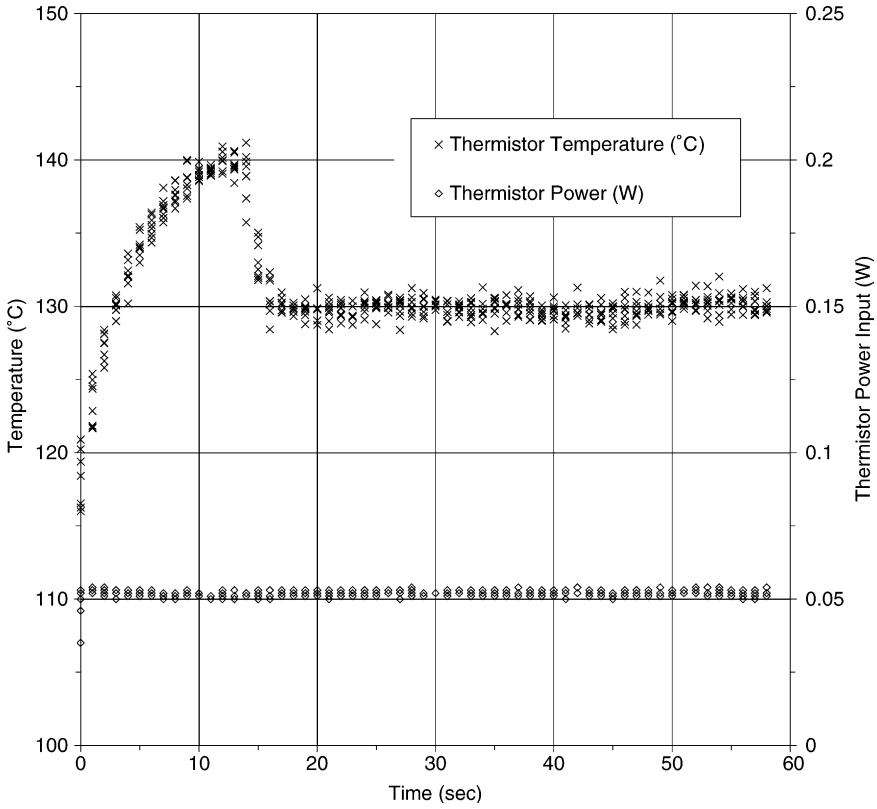

Fig. 3. Sample data from STS-78 LMS Mission. BDPU Pool Boiling. Test PB-31.

and two outer layers without heat generation. The boundary-value heat conduction problem was solved by means of the method of variables and by construction of orthogonal expansions of functions over multi-layer regions, for the case with perfect thermal contact between the layers. The materials for each of the three layers are silicon, glass, and fluid R-123, from the center in turn, and denoted as 1, 2, and 3 in Fig. 2.

The boundary-value problem of heat conduction becomes:

$$0 \leqslant r \leqslant r_1 : \alpha_1 \frac{1}{r^2}\frac{\partial}{\partial r}\left(r^2 \frac{\partial \theta_1}{\partial r}\right) + \frac{\alpha_1}{k_1} g = \frac{\partial \theta_1}{\partial t}(r,t) \tag{1}$$

$$r_1 \leqslant r \leqslant r_2 : \alpha_2 \frac{1}{r^2}\frac{\partial}{\partial r}\left(r^2 \frac{\partial \theta_2}{\partial r}\right) = \frac{\partial \theta_2}{\partial t}(r,t) \tag{2}$$

$$r_2 \leqslant r \leqslant r_3 : \alpha_3 \frac{1}{r^2}\frac{\partial}{\partial r}\left(r^2 \frac{\partial \theta_3}{\partial r}\right) = \frac{\partial \theta_3}{\partial t}(r,t) \tag{3}$$

with the boundary conditions:

$$\frac{\partial \theta_1}{\partial r}(0,t) = 0 \tag{4}$$

$$\theta_1(r_1,t) = \theta_2(r_1,t) \tag{5}$$

$$k_1 \frac{\partial \theta_1}{\partial r}(r_1,t) = k_2 \frac{\partial \theta_2}{\partial r}(r_1,t) \tag{6}$$

$$\theta_2(r_2,t) = \theta_3(r_2,t) \tag{7}$$

$$k_2 \frac{\partial \theta_2}{\partial r}(r_2,t) = k_3 \frac{\partial \theta_3}{\partial r}(r_2,t) \tag{8}$$

$$\theta_3(r_3,t) = 0 \tag{9}$$

and initial conditions

$$\theta_1(r,0) = \theta_2(r,0) = \theta_3(r,0) = 0 \tag{10}$$

Although r_3 in Eq. (9) might have been considered as an infinite domain, it is taken to be sufficiently large relative to r_2 that the temperature gradient at r_3 is negligible, for all practical purposes, and the temperature at that location remains unchanged. The three-composite spherical problem satisfying the boundary and initial conditions here results in the formation of a six-by-six matrix, in which the determinant permits the theoretical determination of the infinite number of eigenvalues and eigenvectors. In the problem addressed here, the first (10) modes were considered sufficient for a reasonable approximation, with each mode having its own eigenvalue and eigenvector. The matrix associated with the present geometry appeared to be difficult to solve due to the so-called ill-matrix. For such a case, a special treatment was applied by multiplying the matrix appropriately with numbers to make the elements of the ill-

Table 1
Summary of selected nucleation data from STS-78 LMS Mission pool boiling

Grp # {1}	BDPU-LMS-nucleation data-large spot heater									Calculated-large spot heater		
	Local test	Pressure	T_{sat}	T_{bulk}	T_{sub}	Input power	T_i^*	$T_{i\,sup}^*$	t^*	K	T_i^*	$T_{i\,sup}^*$
	No. {2}	Bar {3}	°C {4}	°C {5}	K {6}	W {7}	°C {8}	°K {9}	s {10}	$(ms)^{-1}$ {11}	°C {12}	°K {13}
1	PB-31	10.635	114	108.8	5.2	0.052	141.2	27.2	13.9	6.829E+13	145.9	31.9
1	PB-33	8.46	103.2	98.8	4.4	0.104	146.6	43.4	5	1.065E+14	145.6	42.4
2	PB-24	1.36	36.2	33.9	2.3	0.085	86	49.8	10.8	6.514E+12	89.1	52.9
2	PB-64	1.58	40.7	38.9	1.8	0.057	84.4	43.7	20.3	4.516E+12	85.0	44.3
2	PB-79	1.57	40.5	38.9	1.6	0.057	75.8	35.3	12.2	2.313E+13	77.7	37.2
2	PB-82	1.57	40.5	38.8	1.7	0.067	81.9	41.4	12.1	1.189E+13	84.3	43.8
3	PB-66	1.79	44.5	39	5.5	0.057	80.4	35.9	15	2.274E+13	80.8	36.3
3	PB-80	1.78	44.3	38.9	5.4	0.058	78.1	33.8	13	3.423E+13	79.4	35.1
4	PB-30	9.6	109.1	108.4	0.7	0.155	159	49.9	2.3	3.152E+14	151.7	42.6
4	PB-32	7.665	98.8	98.8	0	0.053	130	31.2	9.2	8.971E+13	131.0	32.2
4	PB-34	6.1	88.9	88.8	0.1	0.105	135.8	46.9	5	5.039E+13	136.1	47.2
5	PB-7	2.86	59.9	58.5	1.4	0.11	109	49.1	5	4.135E+13	108.0	48.1
5	PB-38	5.09	81.5	78.7	2.8	0.055	112.5	31	12.6	3.888E+13	116.6	35.1
5	PB-42	2.85	59.8	48.9	10.9	0.099	100	40.2	6	1.341E+14	98.0	38.2
	PB-35	6.96	94.5	88.9	5.6	0.053	123	28.5	21.9	1.262E+13	132.7	38.2
	PB-37	7.94	100.3	78.8	21.5	0.079	133.6	33.3	39.1	1.804E+12	153.8	53.5
	PB-40	3.94	71.5	68.5	3	0.13	115.7	44.2	5.3	2.046E+13	128.9	57.4

matrix uniform. The details of the process are beyond the scope of this presentation. The calculations were performed successfully using a mathematical tool, such as MathCad. The computed temperature rise is defined for convenience as $\theta_i = T_i - T_\infty$, where $i = 1,2,3$.

The solution of the boundary-value problem of the heat conduction becomes:

$$\theta_1(r,t) = \sum_{n=1}^{M} \exp(-\beta_n^2 t) X_{1n} \frac{P}{VN_n} \times \int_0^{r_1} X_{1n} r^2 \,\mathrm{d}r \int_0^t \exp(\beta_n^2) t \,\mathrm{d}t \tag{11}$$

$$\theta_2(r,t) = \sum_{n=1}^{M} \exp(-\beta_n^2 t) X_{2n} \frac{P}{VN_n} \times \int_0^{r_1} X_{1n} r^2 \,\mathrm{d}r \int_0^t \exp(\beta_n^2) t \,\mathrm{d}t \tag{12}$$

$$\theta_3(r,t) = \sum_{n=1}^{M} \exp(-\beta_n^2 t) X_{3n} \frac{P}{VN_n} \times \int_0^{r_1} X_{1n} r^2 \,\mathrm{d}r \int_0^t \exp(\beta_n^2) t \,\mathrm{d}t \tag{13}$$

where

$$X_{1n} = C_{1n}\left(\frac{1}{r}\sin\left(\frac{\beta_n r}{\sqrt{\alpha_1}}\right)\right) + D_{1n}\left(\frac{1}{r}\cos\left(\frac{\beta_n r}{\sqrt{\alpha_1}}\right)\right) \tag{14}$$

$$X_{2n} = C_{2n}\left(\frac{1}{r}\sin\left(\frac{\beta_n r}{\sqrt{\alpha_2}}\right)\right) + D_{2n}\left(\frac{1}{r}\cos\left(\frac{\beta_n r}{\sqrt{\alpha_2}}\right)\right) \tag{15}$$

$$X_{3n} = C_{3n}\left(\frac{1}{r}\sin\left(\frac{\beta_n r}{\sqrt{\alpha_3}}\right)\right) + D_{3n}\left(\frac{1}{r}\cos\left(\frac{\beta_n r}{\sqrt{\alpha_3}}\right)\right) \tag{16}$$

$$N_n = \frac{k_1}{\alpha_1}\int_0^{r_1} X_{1n}^2 r^2 \,\mathrm{d}r + \frac{k_2}{\alpha_2}\int_{r_1}^{r_2} X_{2n}^2 r^2 \,\mathrm{d}r + \frac{k_3}{\alpha_3}\int_{r_2}^{r_3} X_{3n}^2 r^2 \,\mathrm{d}r \tag{17}$$

$$V = \frac{4}{3}\pi r_1^3 \tag{18}$$

β_n is the eigenvalues for non-trivial solution of the 6×6 matrix, which in general is a transcendental equation. For each eigenvalue, the coefficient C_{in} and D_{in} are determined.

By taking derivative of $\theta_3(r,t)$ with respect to r, we have

$$\frac{\partial\theta_3}{\partial r}(r,t) = \sum_{n=1}^{M} \exp(-\beta_n^2 t) X'_{3n} \frac{P}{VN_n} \int_0^{r_1} X_{1n} r^2 \,\mathrm{d}r \times \int_0^t \exp(\beta_n^2) t \,\mathrm{d}t \tag{19}$$

where

$$X'_{3n} = C_{3n}\left(\frac{-1}{r^2}\sin\left(\frac{\beta_n r}{\sqrt{\alpha_3}}\right) + \frac{1}{r}\cos\left(\frac{\beta_n r}{\sqrt{\alpha_3}}\right)\frac{\beta_n}{\sqrt{\alpha_3}}\right) + D_{3n}\left(\frac{-1}{r^2}\cos\left(\frac{\beta_n r}{\sqrt{\alpha_3}}\right) - \frac{1}{r}\sin\left(\frac{\beta_n r}{\sqrt{\alpha_3}}\right)\frac{\beta_n}{\sqrt{\alpha_3}}\right) \tag{20}$$

By taking derivative of $\theta_3(r,t)$ with respect to t, we have

$$\frac{\partial\theta_3}{\partial t}(r,t) = \sum_{n=1}^{M}\left[1 - \beta_n^2 \exp(-\beta_n^2 t)\int_0^t \exp(\beta_n^2) t \,\mathrm{d}t\right] \times X_{3n}\frac{P}{VN_n}\int_0^{r_1} X_{1n} r^2 \,\mathrm{d}r \tag{21}$$

Using Eqs. (11)–(13) with the properties and dimensions in Table 2, for the heater power of 0.05 W and $t^* = 13.9$ s of Fig. 3, corresponding to Local Test no. PB-31 in Table 1, the results of the computation of the temperature distributions surrounding the heater for the three regions are shown in Fig. 4. By presenting the temperature in terms of superheat above the prevailing saturation temperature, the superheat or subcooling in the surrounding liquid can be readily ascertained. The temperature variation across the thermistor heater appears to be negligible for this size, and justifies the use of a uniform heater temperature. The transient superheat of the thermistor, and of the surface of the glass coating of r_2, computed from Eqs. (11) and (12), are given in Fig. 5 as a function of time, with the measured nucleation time as indicated. The temperature drop across the glass coating is computed to be 1.4 K at this time, as may also be see in Fig. 5. It can be noted from Table 1 (for Local Test no. PB-31) that the difference between the measured and computed thermistor superheats at nucleation (columns [8] and [12], respectively) is 4.7 K. This discrepancy can be attributed to the difference between the actual geometry of the thermistor, seen in Fig. 1, and the spherical shape assumed for convenience in the analysis.

Table 2
Properties and dimensions used in calculation

	Radius (mm)	k (W/m K)	ρ (kg/m^3)	C (J/kg K)	$\alpha \times 10^6$ (m^2/s)
Spot heater	$r1 = 0.5$	148	2330	712	89.2
Glass	$r2 = 0.78$	0.7	5000	500	0.28
R-123	$r3 = 5.0$	0.0782	1459	1022	0.0524

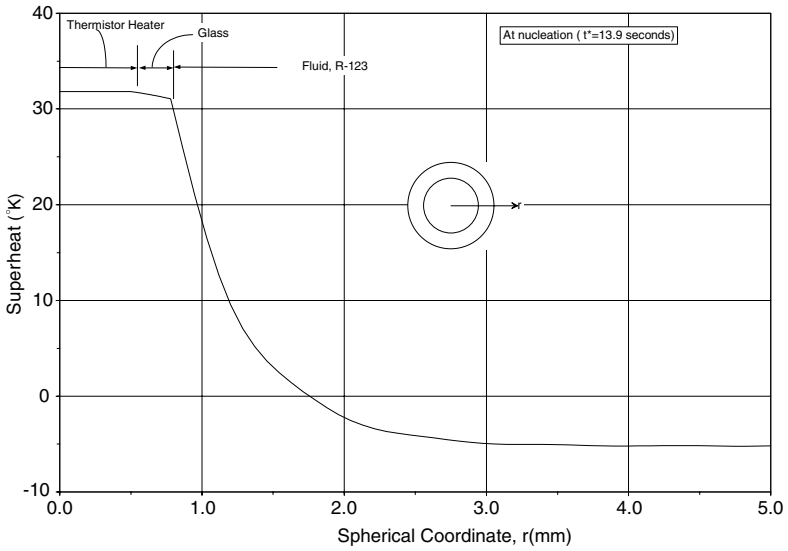

Fig. 4. Predicted radial temperature rise distribution in R-123 at $t^* = 13.9$ s. Test PB-31.

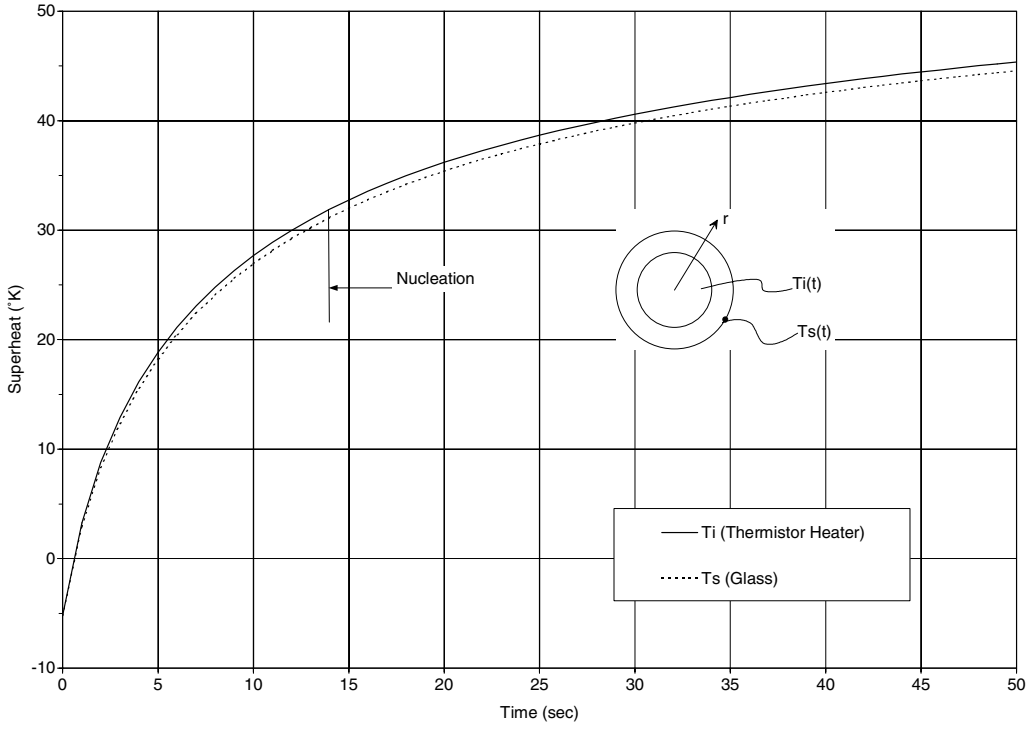

Fig. 5. Predicted transient temperature rise of thermistor heater and surface of glass enclosure. Test PB-31.

4. Kinetics of nucleation

The role of the heat flux or temperature gradient in the liquid at the heater surface, as well as the rate of change of heater surface temperature in addition to the heater surface temperature itself, was examined by Merte and Lee [7] for the description of the quasi-homogenous nucleation process observed to take place on a flat surface acting as a heater in microgravity. This work will be summarized below, taking into account the

change in heater surface geometry from a plane to a spherical surface.

The classical theory of homogenous nucleation provides the steady state nucleation rate, the number of nuclei formed per unit volume and per unit time, and has been described in the works of Volmer [14], Kagen [5], Blander and Katz [2], and more recently with application to hydrocarbons by Kwak and Lee [6]. The expression in each converge approximately to:

$$J = N_{\mathrm{l}}\left(\frac{\sigma}{\pi m B}\right)^{\frac{1}{2}} \exp\left(\frac{-16\pi\sigma^3}{3kT(P_{\mathrm{v}}-P_{\mathrm{l}})^2}\right) \tag{22}$$

Here B is an arbitrary constant that possesses usually 1/3. N_{l} is the number density of liquid molecules. Eq. (22) can be rewritten in a simple form for convenience:

$$J = C\exp(-G) \tag{23}$$

where

$$C = N_{\mathrm{l}}\left(\frac{\sigma}{\pi m B}\right)^{\frac{1}{2}} \tag{24}$$

and G is the dimensionless ratio of the work of formation of a critical size bubble nucleus and kT, the mean molecular fluctuation energy per degree of freedom. This was termed the Gibbs number by Skripov [10], defined as:

$$G = \frac{16\pi\sigma^3}{3kT(P_{\mathrm{v}}-P_{\mathrm{l}})^2} \tag{25}$$

Several different forms for C in Eq. (24) have been proposed, as discussed by Merte and Lee [7], each of which are essentially constant, but differ by two orders of magnitude.

In a manner similar to that given by Skripov [10], the homogeneous nucleation is considered to take place within a distance from the solid heater surface on the order of the size of the embryo bubble at the thermodynamic equilibrium, the so-called critical size. A consequence of this is that the curvature of a realistic sized solid spherical heater can be neglected, except for its effect on the heater surface heat flux, and the analysis for a plane heater surface in Merte and Lee [7] used to estimate the number of embryo bubbles formed, which result in the onset of nucleate boiling.

The number of nuclei formed within a time τ and within a distance x from the heater surface is given by (using the plane approximation):

$$n'' = \frac{n}{A} = \int_0^{\tau}\int_0^{x} J\,\mathrm{d}x\,\mathrm{d}t \tag{26}$$

where J is given by Eq. (23).

The Gibbs number G in Eq. (25) is a function of liquid temperature, following substitution of the Clausius–Clapyron equation and an appropriate expression for the surface tension, and is thus also a function of time and space, as:

$$G(T) = G[T(x,t)] \tag{27}$$

Expanding $G(T)$ into a Taylor series according to powers of $T(\tau,0)$, followed by successive substitution into Eqs. (23) and (26), and integration of Eq. (26), results in:

$$n'' = -\frac{C\exp[-G(0,\tau)]}{G_{\mathrm{T}}^2 T_x \dot{T}} \tag{28}$$

It should be noted that $G_{\mathrm{T}} = \frac{\mathrm{d}G}{\mathrm{d}T}$, $T_x = \frac{\partial T}{\partial x}$ and $\dot{T} = \frac{\partial T}{\partial t}$. Details of the above can be found in Merte and Lee [7].

The numerator of Eq. (28) represents $J(0,\tau)$ evaluated at the heater surface conditions at the moment of nucleation. A constant K is introduced and denoted as J divided by n''.

$$K = \frac{J}{n''} = -G_{\mathrm{T}}^2 T_x \dot{T} \tag{29}$$

It is noted that Eq. (29) no longer contains the coefficient (C) in Eq. (23), and its form is of no consequence as long as it can be approximated as constant for any particular circumstances. T_x and $\dot{T}$ can be calculated for the spherical geometry case by Eqs. (19) and (21), respectively, and G_{T} can be obtained by taking the derivative of $G(T)$ in Eq. (27) with respect to T.

G_{T}^2, T_x and $\dot{T}$ in Eq. (29) are computable values at given conditions of time, heater size and power input, and provide the possibility to estimate the nucleation rate (J) with the assumption that at least one bubble per unit area is needed for n''. Values of the three terms on the right hand side of Eq. (29) are listed in Table 3 for the experimentally imposed parameters of three selected tests, along with their product, K. It is noted that the absolute magnitude of K, which represents the ratio of the volumetric nucleation rate to the unity number of nuclei per unit heater surface area, depends predominantly on (G_{T}), whereas the relative magnitudes depend more on T_x and $\dot{T}$, which depend in turn on the level of heat flux and the length of the heating time up to nucleation, respectively.

Table 3
Comparisons of computed values of G_{T}^2, T_x and $\dot{T}$ for three tests chosen from Table 1

Test run	Power (W)	Delay time (t^*)	T^* (°C)	G_{T}^2	T_x	$\dot{T}$	$K(=J/n'')$
PB-31	0.052	13.9	144.4	1.1×10^9	6.6×10^4	0.943	6.829×10^{13}
PB-82	0.067	12.1	82.3	1.0×10^8	8.3×10^4	1.416	1.189×10^{13}
PB-30	0.155	2.3	148.8	2.1×10^8	1.2×10^5	12.24	3.152×10^{14}

5. Results and discussion

Of the 84 sets of data available from the BDPU pool boiling experiments in the STS-78 LMS mission, 17 sets were selected as amenable to analysis for nucleation, due primarily to the distinct drop in the heater temperature that occurs at nucleation. These are tabulated in Table 1, and include the values of K computed from Eq. (29) in Column {11}. The 17 sets of data are divided into five different groups, indicated in Column {1}, based on the approximate levels of the system pressure. In computing K, the surface tension terms in G_T were initially taken as constant at each level of system pressure. Sample computations made later incorporated $\partial\sigma/\partial T$, with negligible effects on the results, particularly in light of other uncertainties, e.g., the non-sphericity of the actual heater.

It is noted in Table 1 that the computed values of K do not appear to vary significantly over all the tests, covering a range of 10^{12}–10^{14} $(\mathrm{m\,s})^{-1}$. As described previously, K qualitatively represents the volumetric nucleation rate (J) for a unity value of n''. If one considers that at least one critical size nucleus per square centimeter is sufficient for the nucleation process to proceed [10], this provides a minimum value of $n'' = 10^4$ nuclei/m^2. Hence, the minimum value of J can be estimated from the known value of K. For example, in Table 1, $K = 6.829 \times 10^{13}$ $(\mathrm{m\,s})^{-1}$ for test PB-31, and results in $J = 6.628 \times 10^{17}$ nuclei/m^3 s. This is within the range of 10^{12}–10^{28} for the nucleation rate for many organic liquids and water [1,4].

Eq. (29) can be written more specifically in terms of the independent variables as:

$$K(\tau) = \frac{J(0,\tau)}{n''} = -\{G_T[T(0,\tau)]\}^2 T_x(0,\tau)\dot{T}(0,\tau) \qquad (30)$$

As described previously, K can be computed explicitly from Eq. (30) for a given τ with the aid of Eqs. (13), (19), (21), and (27). Values of K for $\tau = t^*$ so computed are given for each test in column {11} of Table 1, for the levels of heat flux, system pressure and subcooling used.

Conversely, for given values of K, heat flux, system pressure and subcooling, t^*, the nucleation delay time, and the corresponding heater surface superheat can be computed from these same equations, albeit only implicitly. Noting in Column {11} of Table 1 that the values of K appear to be reasonably uniform, the value of $K = 6.829 \times 10^{13}$ $(\mathrm{m\,s})^{-1}$ of Test PB-31 is selected as

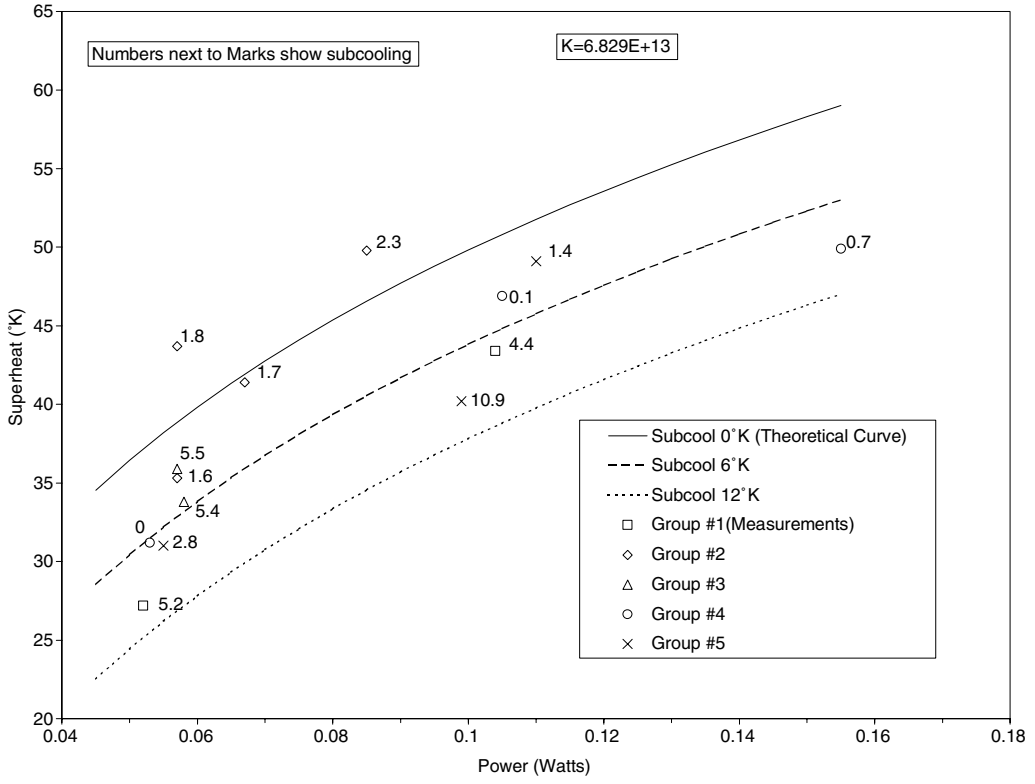

Fig. 6. Predicted thermistor superheat at nucleation from homogeneous nucleation theory for $K = 6.829 \times 10^{13}$ $(\mathrm{m\,s})^{-1}$. Data plotted are measured thermistor superheats from Table 1.

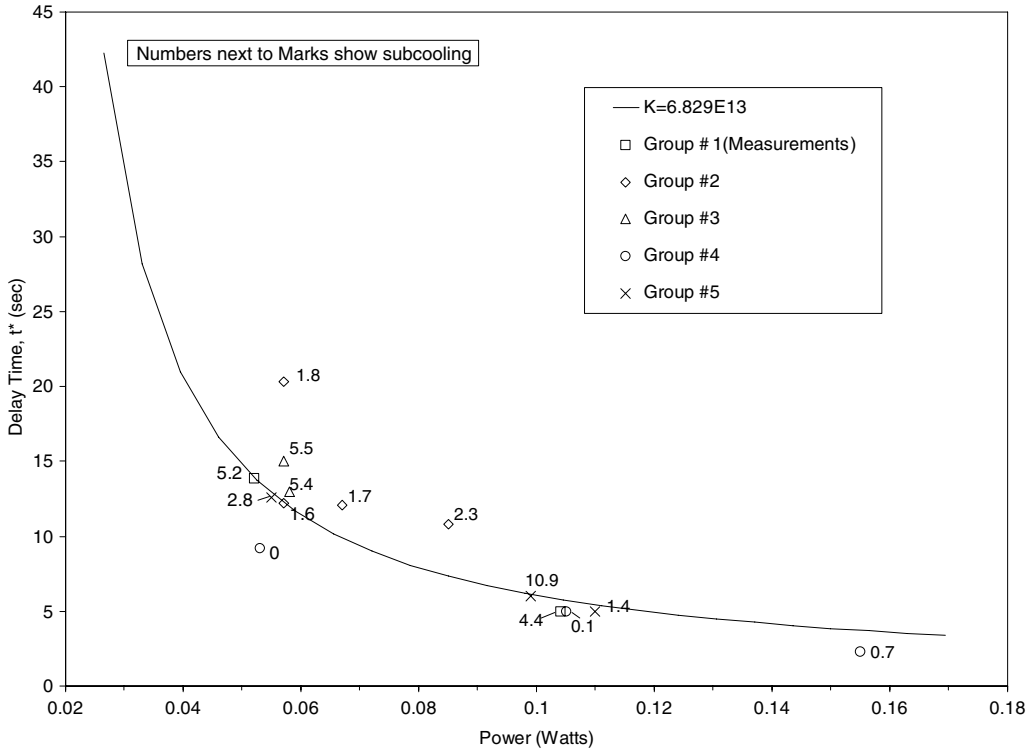

Fig. 7. Theoretical homogeneous nucleation delay time as function of thermistor power input for $K = 6.829 \times 10^{13}$ $(\mathrm{m\,s})^{-1}$. Data plotted are measured delay time (t^*) from Table 1.

typical, for purposes of comparisons between the various tests and the relevant predictions. The heater surface temperature at nucleation is computed by Eq. (13), tabulated in Column {12} of Table 1, and expressed in terms of the corresponding superheat in Column {13}. The measured heater superheat at nucleation (Column {9}) is within 5% of the computed values (Column 13) for all except three tests (PB-35, 37, 40), which have discrepancies of 14%. It should be pointed out that T^* in Table 3 is the surface temperature of the glass layer surrounding the thermistor heater, and is the relevant temperature for nucleation, while T_i^* in Table 1 (column 12) is the computed thermistor temperature at nucleation, for comparison with the measured temperatures in column {8}.

For convenience, the heater superheat is plotted in Fig. 6 as a function of heater power input, for three levels of subcooling which span the range 0–12 K encountered in the experiments. Also included are the measured heater superheats at nucleation, distinguished by symbols according to the groups defined in terms of system pressure, and by the subcooling appearing alongside each data point. It is to be noted that, for the most part, reasonably good qualitative agreement exists between the measurements and predictions in that heater superheat at nucleation increases with power input, and decreases as the subcooling increases. The discrepancies are attributed to the necessary approximation of the heater as a sphere, which includes a uniform glass coating around the heater. The degree to which this is not valid can be judged by examining Fig. 1.

Fig. 7 is a plot of the predicted nucleation delay time (t^*) as a function of the input power with $K = 6.829 \times 10^{13}$ $(\mathrm{m\,s})^{-1}$ of Test PB-31, together with the measurements from Table 1, again distinguished by symbols according to the groups and by the subcooling alongside each data point. It is to be noted that the delay time increases exponentially as the power input decreases, similar to that in the microgravity pool boiling experiments of Merte and Lee [7].

6. Conclusions

A microgravity experiment is particularly advantageous in the study of homogenous nucleation on a spherical shaped heating surface, since the transient temperature distribution is known in the fluid at the moment of nucleation. An analytical model was used to predict the temperature distribution around the spherical heater, making feasible a quantitative determination

of the conditions associated with homogenous nucleation.

The results of the present study are in essential agreement with the quasi-homogenous nucleation results for a plane heating surface developed by Merte and Lee [7]. It is possible, using the nucleation model, to predict the superheat of the heating surface and the delay time of nucleation under given conditions of power input, system pressure, liquid subcooling, and heater radius.

Acknowledgements

The work here is the result of a cooperative arrangement between NASA, under NASA Grant NAG3-1310, ESA, and DLR Grant 50 WM9566. The support of the respective agencies is gratefully acknowledged by the authors.

References

[1] C.T. Avedisian, The homogeneous nucleation limits of liquids, J. Phys. Chem., Ref. Data 14 (3) (1985) 695–729.
[2] M. Blander, J.L. Katz, Bubble nucleation in liquids, AIChE J. 21 (1975) 833–848.
[3] P.E. Bulavin, V.M. Kashcheev, Solution of nonhomogeneous heat-conduction equation for multilayered bodies, Int. Chem. Eng. 5 (1) (1965) 112–115.
[4] V.P. Carey, Liquid–Vapor Phase-Change Phenomena, Taylor and Francis, Hemisphere, Bristol, PA, 1992.
[5] Y. Kagan, The kinetics of boiling of a pure liquid, Russ. J. Phys. Chem. 34 (1960) 42–46.
[6] H.-Y. Kwak, S. Lee, Homogeneous bubble nucleation predicted by a molecular interaction model, J. Heat Transfer 113 (1991) 714–721.
[7] H. Merte Jr, H.S. Lee, Quasi-homogeneous nucleation in microgravity at low heat flux: experiments and theory, J. Heat Transfer 119 (1997) 305–312.
[8] H. Merte Jr., H.S. Lee, R.B. Keller, Dryout and rewetting in the pool boiling experiment flown on STS-72 (PBE-IIB) and STS-77 (PBE-IIA), Final Report NASA Grant NAG-1684, Report no. UM-MEAM-98-01, Department of Mechanical Engineering and Applied Mechanics, The University of Michigan, Ann Arbor, Michigan, January 1998.
[9] S.S. Sadhal, P.S. Ayyaswamy, J.N. Chung, Transport Phenomena with Drops and Bubbles, Springer-Verlag, New York, 1997.
[10] V.P. Skripov, Metastable Liquids, Halsted Press, John Wiley & Sons, New York, 1974.
[11] J. Straub, J. Winter, G. Picker, M. Zell, Study of vapor bubble growth in supersaturated liquid, in: Proceedings of the 1995 National Heat Transfer Conference, vol. 3, ASME HTD-Vol. 305, 1995, pp. 29–37.
[12] J. Straub, J. Winter, G. Picker, M. Zell, Boiling on a miniature heater under microgravity—a simulation for cooling of electronic devices, in: Proceedings of the 1995 National Heat Transfer Conference, vol. 3, ASME HTD-Vol. 305, 1995, pp. 61–69.
[13] J. Straub, Boiling heat transfer and bubble dynamics in microgravity, in: Advances in Heat Transfer, vol. 35, Academic Press, New York, 2001, pp. 57–172.
[14] M. Volmer, Kinetics of Phase Change, Steinkopff, J.W. Edwards, Dresden, Ann Arbor, MI, 1939.